Collective enhancement of nuclear level density and its fade-out in ^{161}Dy

T. Santhosh,[1,2,*] P. C. Rout,[1,2,†] S. Santra,[1,2] A. Pal,[1] G. Mohanto,[1] Ramandeep Gandhi,[1,2] and A. Baishya[1,2]
[1]*Nuclear Physics Division, Bhabha Atomic Research Centre, Mumbai-400085, India*
[2]*Homi Bhabha National Institute, Anushaktinagar, Mumbai-400094, India*

(Received 4 July 2023; revised 16 August 2023; accepted 2 October 2023; published 20 October 2023)

The nuclear level density is a fundamental quantity in nuclear physics, governing various nuclear reactions and astrophysical processes. In this study, we report on the collective enhancement of nuclear level density and its fade-out with excitation energy in the deformed ^{161}Dy, obtained through an exclusive measurement of neutron evaporation spectra. The ^{162}Dy nucleus was populated via the transfer of a triton in a ^{7}Li-induced reaction on ^{159}Tb. Statistical model analysis of the neutron spectra revealed a large collective enhancement factor of 42±2, consistent with microscopic calculations. This enhancement factor is similar to the one obtained for mass $A \sim 170$ in our previous measurement. The energy-dependent collective enhancement over a wide range of excitation energies was inferred by combining the present results with the available Oslo level density below the neutron binding energy.

DOI: 10.1103/PhysRevC.108.044317

I. INTRODUCTION

The atomic nucleus poses a complex many-body problem, compounded by a limited understanding of the fundamental internucleon interaction. To establish a correlation between experimental data and develop a more comprehensive theory, simplified models such as the shell model and the rotational model have been proposed [1,2]. The equilibrium shape of a nucleus is deformed due to its shell structure, which, in turn, is linked to its rotational degrees of freedom. Given the complexity of nuclear forces and the large number of degrees of freedom involved, symmetry properties play a crucial role in characterizing nuclear states. One important aspect of nuclear states is the nuclear level density (NLD), defined as the number of levels per unit MeV energy, which is crucial for predicting and interpreting the outcomes of many nuclear reactions. The NLD plays a key role in describing the thermodynamic properties of an excited nucleus, such as temperature and entropy, as well as the decay probabilities of particle emissions from compound nuclear processes using statistical models [3]. This makes NLD relevant in estimating low energy astrophysical reaction rates [4,5], studying giant resonances [6], and determining reaction rates relevant to energy and isotope production in medical applications [7].

Understanding NLD involves investigating various aspects. These include the role of shell effects and nuclear deformation [8,9], temperature-dependent behavior, the influence of nuclear structure and pairing correlations [10], the impact of nuclear reactions, and the connection to astrophysical processes. By studying these factors, we can gain insights into the fundamental nature of NLD and its implications in nuclear physics and astrophysics.

By considering the nucleus as a collection of noninteracting fermions, Bethe [11] derived the level density formula and expressed it as

$$\rho(E_x) = \frac{1}{12\sqrt{2}\sigma} \frac{\exp\left(2\sqrt{aE_x}\right)}{a^{1/4}E_x^{5/4}}, \tag{1}$$

where E_x is the excitation energy of the nucleus and $\boldsymbol{a}$ is the level density parameter with $a = \pi^2 g/6$, $\boldsymbol{g}$ is the single-particle level density evaluated at the Fermi energy. However, this expression does not consider the observed variations in level densities for different types of nuclei (even-even, odd-even, even-odd, and odd-odd). Bethe formula is a good approximation for explaining the NLD at high excitation energy. However, it becomes inadequate at low energy due to the dominance of nuclear structure effects, such as shell effects and collective excitations, and pairing correlations. Several subsequent works have aimed to include these effects in the level density parameter $\boldsymbol{a}$ and excitation energy $\boldsymbol{E_x}$. The correction in excitation energy is referred to as the back-shifted Fermi gas (BSFG) model [12]. Another widely used model for describing experimental NLD at low energy is the constant temperature model [13]. More recently, microscopic models such as Hartree-Fock-Bardeen Cooper Schrieffer [14], HF-Bogoliubov with combinatorial method [15], and shell model Monte Carlo [16,17], have been successful in accurately predicting NLD at low energy ranges, taking into account correlations and structure effects.

To gain more insight into nuclear rotational motion, one can investigate NLDs at excitation energies where statistical principles can be utilized. If collective rotational motion is present, it suggests that there are more degrees of freedom

*tsanthu@barc.gov.in
†prout@barc.gov.in

for low-energy excitations, which could result in a substantial increase in the total NLD.

Collective effects are a natural occurrence when extracting microscopic level density. However, phenomenologically, these effects can also be introduced explicitly by incorporating collective enhancement factors into an intrinsic Fermi gas level density. For a deformed nucleus, a large contribution from collective states, known as collective enhancement, is anticipated in addition to the intrinsic level density. The total level density for a deformed nucleus can be expressed as

$$\rho_{\text{tot}} = \rho_{\text{int}} K_{\text{vib}} K_{\text{rot}}, \tag{2}$$

where K_{vib} and K_{rot} represent the vibrational and rotational enhancement factors, respectively. The contribution from vibrational states is limited due to their large energy spacings, accounting for only a small factor of $\sim$2 of the total level density in a fully deformed nucleus.

To obtain the level density for a specified spin J of an axially symmetric deformed nucleus, the intrinsic states with specified K (spin projection on the symmetry axis) are summed over

$$\rho(E_X, J) = \sum_{K=-J}^{J} \frac{1}{\sqrt{8\pi}\sigma_\perp} e^{\frac{-K^2}{2\sigma^2}} \rho_{\text{int}}(E_X - E_{\text{rot}}). \tag{3}$$

This level density was obtained in the earlier works of Bohr, Mottelson, and Björnholm for an axially symmetric deformed nucleus and resulted in a factor of $\sigma_\perp^2$ higher than for a spherical nucleus. $\sigma_\perp$ is the perpendicular spin cut-off parameter that describes the width of the spin distribution along the perpendicular axis. For Lanthanides, $\sigma_\perp \approx 11\sqrt{T\,(\text{MeV})}$, which implies a rotational enhancement factor of around 100 at nucleon binding energies.

As the excitation energy of the nucleus increases, the strength of the coupling between the intrinsic and collective states also increases. However, this coupling eventually dilutes the collective nature of the levels over the neighboring intrinsic states. This leads to the fading out of the collective enhancement at high excitation energies. Experimental studies have been carried out to observe this phenomenon, including measurements of nuclear level densities, γ-ray strength functions, and other related observables.

In the past, Jhungans *et al.* [18], in a projectile fragmentation experiment, pointed out the necessity for the inclusion of collective enhancement to explain the observed experimental data. On the contrary, in the work of Komarov *et al.* [19], no fade-out of enhancement was observed in the region studied. Recently many experimental observations [20–22] confirmed the collective enhancement of NLD and its fade-out although the measured magnitude of enhancement does not match with the theoretical predictions. The observed collective enhancement factor is roughly about $\sim$8–10 and fade-out happened around $\sim$14 MeV.

In our recent measurement [23], we have inferred the collective enhancement of NLD in the deformed ^{171}Yb nucleus, along with its fade-out with excitation energy. This inference was made through an exclusive measurement of neutron spectra. The statistical model analysis of these spectra revealed a significant collective enhancement factor of 40 ± 3, which is consistent with recent microscopic model predictions but stands out as an anomalous result compared to measurements in nearby deformed nuclei. Importantly, we highlight the significance of the large collective enhancement in the radiative neutron capture cross section, which holds astrophysical relevance. These findings emphasize the importance of further experimental investigations to refine our understanding of collective enhancement in NLD and its potential impact on nuclear reactions.

The present work focuses on the determination of the nuclear level density of ^{161}Dy, which is produced through an incomplete fusion reaction using weakly bound ^{7}Li projectiles. The ^{7}Li nucleus has a cluster structure with a dominant reaction mechanism of breakup or transfer capture of one of the clustered parts to the target nucleus. In this case, the ^{7}Li nucleus is mainly composed of an α particle and a triton, and triton transfer or breakup fusion is the dominant process during an incomplete fusion reaction. The compound nucleus ^{162}Dy was populated by capturing a triton in the ^{159}Tb nucleus. The NLD was then extracted by measuring the evaporated neutron spectra from ^{162}Dy.

II. EXPERIMENTAL DETAILS

The experiment was carried out at the BARC-TIFR 14UD Pelletron laboratory at Mumbai. A pulsed ^{7}Li beam [width $\sim$1.5 ns (FWHM) and period $\sim$107 ns] with an energy of 40 MeV was directed at a self-supported ^{159}Tb target, which had a thickness of 2.8 mg/cm^2. The target thickness was determined using weighing and was mounted on stainless steel frames. A blank frame was also employed to estimate any scattering caused by the beam hitting the target ladder. A current integrator was utilized to monitor the total beam incident on the target.

In order to detect the outgoing α particles in the breakup/transfer channel of ^{7}Li, two ΔE-E telescopes (5 cm $\times$ 5 cm) were employed, each consisting of a double-sided silicon strip detector (DSSD). The telescopes were positioned at a distance of 10 cm from the target center, at an average angle of $\pm 60^\circ$ relative to the beam direction. The ΔE and E detectors had thicknesses of 50 μm and 1500 μm, respectively. Each DSSD had 16 strips on each side and covered an angular range of 25°. α particles were identified using the Bethe-Bloch energy loss technique in strip telescopes, these α particles were then used to find the neutrons in coincidence.

Evaporated neutrons from the compound nucleus were detected using an array of 15 liquid scintillation (LS, EJ301) detectors arranged in circular geometry [24]. The detector array was placed 70 cm from the target center at angles ranging from 58° to 143° with respect to the incident ^{7}Li beam. The standard pulse-shape discrimination (PSD) technique was used for unambiguous detection of neutrons against γ rays. Neutron energy spectra were determined using the time-of-flight (TOF) method, which involved measuring the time taken for neutrons to travel from the target to the detectors using the pulsed beam bunched with a period of approximately 107 ns.

All signal readouts from LS detectors and strip detectors had been recorded in list mode using a Versa Module

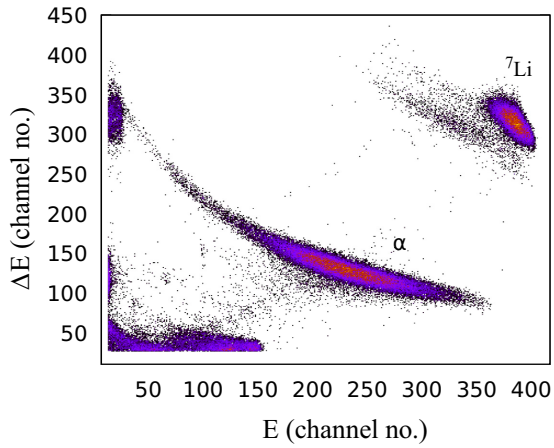

FIG. 1. A standard 2D plot illustrating the energy loss of particles in one of the strips of a ΔE-E telescope.

Europa based data acquisition system. A shadow pyramid bar of iron plates was kept in front of the LS detector array to estimate the scattered neutron contribution from the surroundings. The beam dump was shielded with borated paraffin and lead blocks to reduce the background.

A typical two-dimensional (2D) plot of the energy loss of particles in the ΔE and E strip detectors for one of strips is shown in Fig. 1. It is observed that the α particles are well separated from ^{7}Li. The PSD in relation to the TOF for the ^{7}Li + ^{159}Tb reaction is displayed in the top panel of Fig. 2, while the bottom panel depicts the TOF spectra gated with α particles. To extract the absolute neutron TOF, the prompt γ signal illustrated in Fig. 2 was used as a reference. The inset in Fig. 2 shows the α energy distribution peaking at ∼22 MeV, which corresponds to the energy of the beam velocity. Different energy bins were identified to obtain the neutron spectra for various excitation energies. The neutron TOFs were subsequently converted into neutron energy spectra using appropriate Jacobian factor. The efficiency of neutron detectors as a function of incident energy and threshold were estimated using a Monte Carlo simulation [24], which was validated using measured neutrons from ^{7}Li(p, n) reaction. The efficiency corrected neutron energy spectra after converting into the center of mass are shown in Fig. 3. In the center of mass frame, it is also observed that the forward and backward spectra exhibit symmetry around 90°. This symmetry implies that the emission of neutrons originates from a statistically equilibrated system.

III. RESULTS AND DISCUSSION

In order to quantify the collective enhancement, if at all reflected in the neutron spectra, we compared the experimentally measured neutron spectra with statistical model code CASCADE [26]. The code has been very successful in explaining the evaporation spectra. The following E_X and J dependent level density expression has been used in the CASCADE code,

$$\rho(E_x, J) = \frac{(2J+1)\sqrt{a}}{12U^2}\left(\frac{\hbar^2}{2\Im}\right)^{3/2} e^{2\sqrt{aU}}, \qquad (4)$$

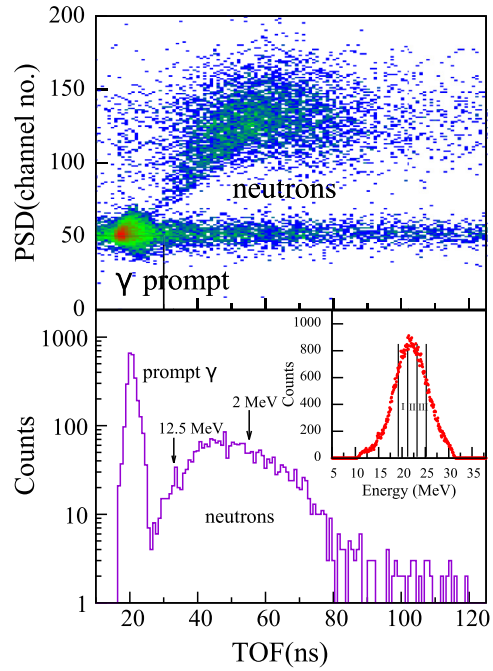

FIG. 2. (Top) The pulse shape discrimination (PSD) as a function of time of flight (TOF) in the ^{7}Li + ^{159}Tb reaction. The prompt γ rays and neutrons are clearly separated. (Bottom) A typical TOF in the ^{7}Li + ^{159}Tb reaction, specifically for the central energy bin of α particles. Two representative neutron energies are indicated by arrows, highlighting their positions in the TOF spectrum. The inset in the figure displays the projected α energy spectrum with three energy bins indicated for reference.

where U is defined as $U = E_X - E_{\rm rot} - \Delta_P$, with Δ_P being the pairing energy calculated using $\Delta_P = \frac{12}{\sqrt{A}}$ and $E_{\rm rot}$ representing the rotational energy given by $E_{\rm rot} = (\frac{\hbar^2}{2\Im})J(J+1)$, where $\Im$ denotes the moment of inertia defined as $\Im = I_0(1 + \delta_1 J^2 + \delta_2 J^4)$ with I_0 being the rigid body moment of inertia, and δ_1, δ_2 representing the deformability parameters of a liquid drop nucleus [27].

The expression for the level density parameter a has been parametrized using the Ignatyuk prescription [28] as $a = \tilde{a}[1 - \frac{\Delta_S}{U}(1 - e^{-\gamma U})]$, where $\tilde{a}$ represents the asymptotic value of the NLD parameter in the liquid drop region. Δ_S denotes the shell correction energy, which is calculated as the difference between the experimental binding energy and the binding energy calculated from the liquid drop model (LDM). γ represents the damping parameter [29].

The CASCADE code has the feasibility to include collective enhancement ($K_{\rm coll}$) explicitly, and is modeled as

$$K_{\rm coll} = 1 + A_{en}(1 + \exp[(E - E_{cr})/d_{cr}])^{-1}, \qquad (5)$$

where A_{en} represents the maximum factor by which enhancement is collectively increased, E_{cr} denotes the energy at which the enhancement decreases to half of its maximum value, and d_{cr} represents the width of the transition region.

Although the statistical model does not consider many details of the nuclear interactions, the empirical parameters determined by the fitting of experimental data reflect the collective enhancement, shell effects, the pairing effects, etc.

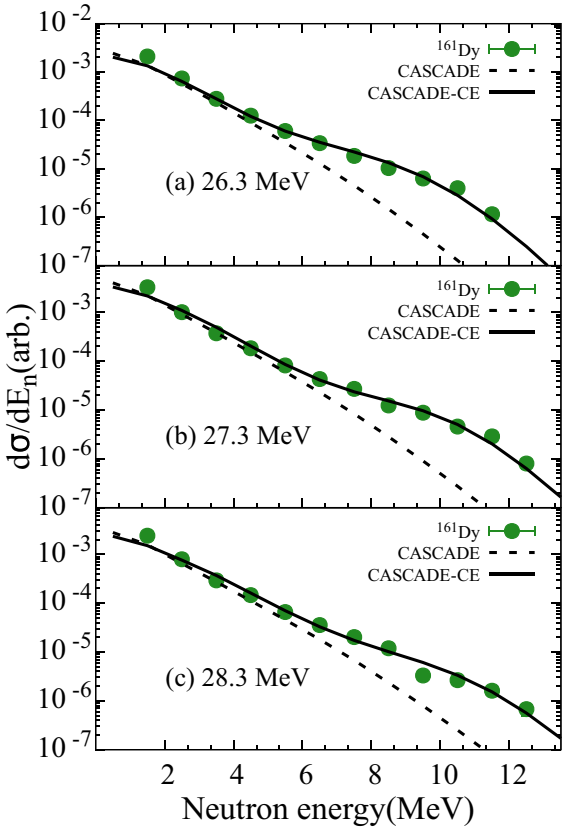

FIG. 3. Comparison of neutron spectra with a statistical model calculation using the level density parameter $A/8.5$ MeV^{-1}. Solid line shows calculation with collective enhancement (CASCADE-CE) and dashed line is without collective enhancement (CASCADE). Three excitation energies (a) 26.3 MeV, (b) 27.3 MeV, and (c) 28.3 MeV, respectively, for three α energy gates (III, II, and I) as shown in inset of Fig. 2.

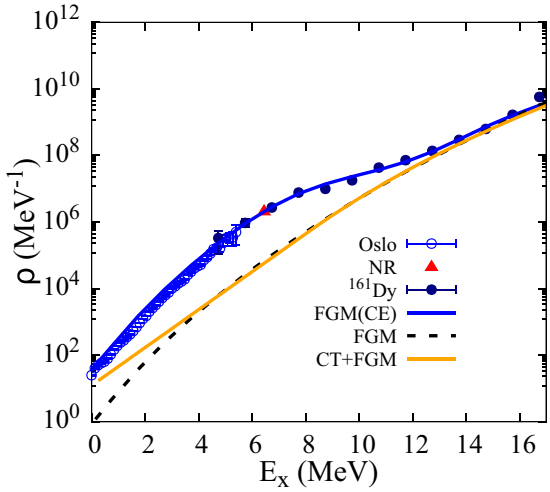

FIG. 4. The normalized level density as a function of excitation energy is depicted in the plot with Oslo data represented by open circles [25] and the present experiment by filled circles. The NLD is normalized to the level density at the neutron resonance point (NR), indicated by a triangle. The dashed red line represents the intrinsic level density from the Fermi gas model (FGM), while the blue solid line represents the Fermi gas level density with collective enhancement [FGM(CE)]. Solid orange line shows the level density from constant temperature + Fermi gas model (CT+FGM).

Figure 3 presents a comparison of neutron spectra obtained at three different excitation energies with CASCADE results. The dashed lines (CASCADE) in the figure represent CASCADE calculations without considering collective enhancement, while solid lines includes this effect (CASCADE-CE). The CASCADE statistical model calculation matches the low-energy neutron part, which has a constant slope, and collective enhancement is added to reproduce the experimental results. This is achieved by adjusting the inverse level density parameter k (defined as $k = A/a$) and collective enhancement function parameters (A_{en}, E_{cr}, and d_{cr}) in the CASCADE input. The inverse level density parameter $k = A/8.5$ MeV^{-1} was used in the calculation. The value k was determined by fitting to the low-energy neutron spectra (<6 MeV), and then the enhancement function parameters were subsequently modified to reproduce the experimental data. The best parameters were determined by simultaneously fitting the three excitation energies, yielding a maximum collective enhancement factor of 42 ± 2, and values of E_{cr} and d_{cr} at 8.5 ± 0.5 MeV and 1.2 ± 0.2 MeV, respectively.

One difficulty in extracting the NLD from evaporation spectra is the influence of multiple decay steps. During these decay steps, the evaporated particles sample the NLD of multiple nuclei, resulting in an "average" NLD. However, if particle evaporation is restricted to the first step only, this difficulty can be avoided. In the present case, the excitation energy of ^{162}Dy led to the predominant emission of high-energy neutrons (>5 MeV) in the first step of neutron emission. The CASCADE calculations for $E_X = 27.3$ MeV show that, above 6 MeV, the first step's contribution is more than 80%, and above 8 MeV, it is 100%. This implies that the collective enhancement extracted in this measurement pertains to ^{161}Dy.

Our primary objective is to determine the excitation energy-dependent level density, which cannot be fully extracted from neutron spectra without being influenced by a particular model. To address this issue, a model-independent method has been developed to obtain the total level density. The initial step involves fitting the center-of-mass neutron spectra to a CASCADE calculation that employs the prescribed level density [in the present case Eq. (4)]. Then using this NLD prescription with collective enhancement inclusion we looked for the optimal value of the level density parameter a that provides the best fit to the experimental data. Once these optimal fits are obtained, the total NLD for the residual nucleus following the emission of one neutron at a specific excitation energy is extracted using the expression [30]

$$\rho(E_x) \propto \frac{(d\sigma/dE_n)_M}{(d\sigma/dE_n)_T}\rho_T(E_x). \tag{6}$$

The $\rho_T(E_x)$ was determined by adding up the NLDs that best fit the data for all values of angular momentum. $(d\sigma/dE_n)_M$ and $(d\sigma/dE_n)_T$ are the measured and cascade-predicted differential neutron cross sections, respectively.

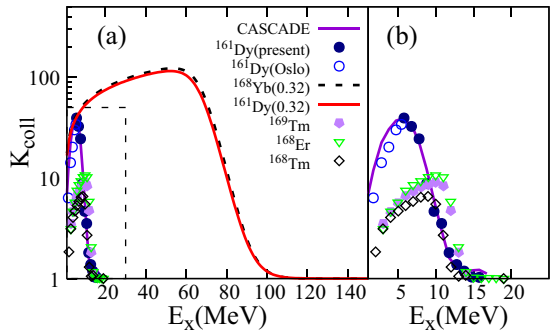

FIG. 5. (a) The enhancement factor as a function of excitation energy, obtained by comparing the level density calculations incorporating Kcoll (collective enhancement) in the CASCADE model to the constant temperature+Fermi gas model (CT+FGM), referred to as CASCADE. Also presented are the combined enhancement extracted from Oslo data along with the present measured enhancement. Experimental enhancement factors for various nuclei [22] are also included. Additionally, the enhancement function extracted from Hansen and Jensen's prescription [32] is showcased for the nuclei ^{168}Yb and ^{161}Dy which have $\beta_2 = 0.32$. (b) Represents the zoomed part of (a) marked in dashed box.

In order to derive the absolute total nuclear level density of ^{161}Dy as a function of excitation energy, the relative nuclear level density $\rho(E_x)$ was modified by normalizing it with the level density 2.1×10^6 MeV^{-1} obtained from neutron resonance data [31] at the neutron binding energy 6.45 MeV. The resulting data were then merged with the level density data obtained via the Oslo method to generate a comprehensive overview covering the energy range from above zero to 16 MeV. Figure 4 illustrates that the level density increases as the excitation energy increases with complete fade-out occurring around 15 MeV.

Figure 5 shows the enhancement factor as a function of excitation energy extracted from the ratio of level density with Kcoll (collective enhancement) included in the CASCADE calculations to the Fermi gas model + constant temperature model (CT+FGM), denoted as CASCADE. The enhancement extracted from Oslo data combined with present measured enhancement is also shown. These are extracted by taking the ratio between experimental level density and CT+FGM level density. Experimental enhancement factors extracted for various nuclei are plotted as well. Additionally, the enhancement function extracted from the Hansen and Jensen's prescription [32] for the nuclei ^{168}Yb and ^{161}Dy is included. The plot provides the collective enhancement behavior with respect to excitation energy, highlighting the significance of different modeling approaches and experimental measurements in understanding the underlying physics of nuclear excitations.

The potential sources of uncertainty in the current measurement are outlined as follows. In cases where the target material contains impurities such as carbon and oxygen, there may be a significant presence of background neutrons. Although these impurities may only constitute a small fraction of the material's weight, their impact can be amplified by the characteristics of the neutron spectra for light targets and kinematic focusing at forward angles. As a result, measurements are often limited to backward angles, especially for high-energy neutron spectra of interest. However, this restriction does not affect the determination of the NLD as pre-equilibrium nuclear reactions are more significant at forward angles and are not as relevant at low beam energies, as is the case in the current measurement. In the present measurement, although the triton breakup/transfer-fusion reaction is expected to be the primary contributor to the coincident neutron spectra, there are other direct processes that could also play a role. However, we can safely disregard the proton pickup and two-neutron transfer cross sections as their contribution is negligible [33]. The most significant reaction to consider is the deuteron transfer followed by ^{5}He breakup. However, since the spectroscopic factor for the $d + {}^5$He configuration is anticipated to be much smaller than that of the $t + {}^4$He configuration, the contribution of this reaction is insignificant [34].

IV. CONCLUSION

In conclusion, our study utilized an incomplete fusion reaction to investigate the compound nucleus of ^{162}Dy and observed the resulting neutron evaporation spectra. By employing the statistical model calculations and comparing with experimental data, we found a significant deviation between standard statistical model calculations and experimental results, indicating the presence of collective enhancement. To address this discrepancy, we proposed an excitation energy-dependent collective enhancement based on Hansen and Jensen's suggestion. Incorporating this collective enhancement, we were able to successfully explain the experimental data. Furthermore, our statistical model analysis revealed a maximum collective enhancement of 42 ± 2 with fade-out observed at around 15 MeV. These results are in agreement with the recent microscopic calculations. Recent theoretical works on NLD using the finite-temperature relativistic Hartree-Bogoliubov model [35] showed that the enhancement in the mass region $A = 160$–170 is ≈ 40. In another work [36], using a microscopic level density model, a similar magnitude of collective enhancement has been predicted. The energy-dependent collective enhancement was inferred by combining our results with Oslo level density data below the neutron binding energy, providing insights into the behavior of collective enhancement over a wide range of excitation energies. These findings highlight the importance of considering collective enhancement in statistical model calculations for describing compound nucleus reactions and provide valuable information for further studies in nuclear reaction dynamics.

ACKNOWLEDGMENTS

We thank B. K. Nayak and D. R. Chakrabarty for their valuable comments and suggestions. We thank the PLF staff for smooth operation of the accelerator. T.S. (IF180174) is sincerely grateful to DST for financial support under the DST-INSPIRE Fellowship scheme.

[1] M. G. Mayer, Phys. Rev. **74**, 235 (1948).
[2] A. Bohr and B. R. Mottelson, *Nuclear Structure*, 1st ed. (Benjamin, Reading, MA, 1969).
[3] T. Ericson, Adv. Phys. **9**, 425 (1960).
[4] T. Rauscher, F. K. Thielemann, and K. L. Kratz, Phys. Rev. C **56**, 1613 (1997).
[5] T. Rauscher and F. K. Thielemann, At. Data Nucl. Data Tables **75**, 1 (2000).
[6] D. R. Chakrabarty, N. Dinh Dang, and V. M. Datar, Eur. Phys. J. A **52**, 143 (2016).
[7] A. Nikjou and M. Sadeghi, Appl. Radiat. Isot. **136**, 45 (2018).
[8] S. K. Kataria, V. S. Ramamurthy, and S. S. Kapoor, Phys. Rev. C **18**, 549 (1978).
[9] S. Bjørnholm, A. Bohr, B. Mottelson, in *Physics and Chemistry of Fission*, Proceedings of a Conference at Rochester (IAEA, Vienna, 1974), Vol. 1, p. 367.
[10] N. Vinh Mau and D. Vautherin, Nucl. Phys. A **445**, 245 (1985).
[11] H. A. Bethe, Phys. Rev. **50**, 332 (1936).
[12] W. D. Myers and W. J. Swiatecki, Lawrence Berkeley Laboratory Report No. LBL-36803, 1994.
[13] A. Gilbert and A. G. W. Cameron, Can. J. Phys. **43**, 1446 (1965).
[14] P. Demetriou and S. Goriely, Nucl. Phys. A **695**, 95 (2001).
[15] S. Hilaire and S. Goriely, Nucl. Phys. A **779**, 63 (2006).
[16] C. Ozen, Y. Alhassid, and H. Nakada, Phys. Rev. Lett. **110**, 042502 (2013).
[17] Y. Alhassid, G. F. Bertsch, C. N. Gilbreth, and H. Nakada, Phys. Rev. C **93**, 044320 (2016).
[18] A. Junghans, M. de Jong, H.-G. Clerc, A. Ignatyuk, G. Kudyaev, and K.-H. Schmidt, Nucl. Phys. A **629**, 635 (1998).
[19] S. Komarov, R. J. Charity, C. J. Chiara, W. Reviol, D. G. Sarantites, L. G. Sobotka, A. L. Caraley, M. P. Carpenter, and D. Seweryniak, Phys. Rev. C **75**, 064611 (2007).
[20] K. Banerjee, P. Roy, D. Pandit, J. Sadhukhan, S. Bhattacharya, C. Bhattacharya, G. Mukherjee, T. Ghosh, S. Kundu, A. Sen, T. Rana, S. Manna, R. Pandey, T. Roy, A. Dhal, M. Asgar, and S. Mukhopadhyay, Phys. Lett. B **772**, 105 (2017).
[21] G. Mohanto, A. Parihari, P. C. Rout, S. De, E. T. Mirgule, B. Srinivasan, K. Mahata, S. P. Behera, M. Kushwaha, D. Sarkar, B. K. Nayak, A. Saxena, A. K. Rhine Kumar, A. Gandhi, Sangeeta, N. K. Deb, and P. Arumugam, Phys. Rev. C **100**, 011602(R) (2019).
[22] Deepak Pandit, B. Dey, S. Bhattacharya, T. K. Rana, D. Mondal, S. Mukhopadhyay, S. Pal, A. De, P. Roy, K. Banerjee, S. Kundu, A. K. Sikdar, C. Bhattacharya, and S. R. Banerjee, Phys. Lett. B **816**, 136173 (2021).
[23] T. Santhosh, P. C. Rout, S. Santra, A. Shrivastava, G. Mohanto, S. K. Pandit, A. Pal, Ramandeep Gandhi, A. Baishya, and Sangeeta Dhuri, Phys. Lett. B **841**, 137934 (2023).
[24] P. C. Rout, A. Gandhi, T. Basak, R. G. Thomas, C. Ghosh, A. Mitra, G. Mishra, S. P. Behera, R. Kujur, E. T. Mirgule, B. K. Nayak, A. Saxena, S. Kumar, and V. M. Datar, J. Inst. **13**, P01027 (2018).
[25] A. Schiller, A. Bjerve, M. Guttormsen, M. Hjorth-Jensen, F. Ingebretsen, E. Melby, S. Messelt, J. Rekstad, S. Siem, and S. W. Odegard, Phys. Rev. C **63**, 021306(R) (2001).
[26] F. Puhlhofer, Nucl. Phys. A **280**, 267 (1977).
[27] S. Cohen, F. Plasil, and W. J. Swiatecki, Ann. Phys. **82**, 557 (1974).
[28] A. V. Ignatyuk, G. N. Smirenkin, and A. S. Tishin, Yad. Fiz. **21**, 485 (1975) [Sov. J. Nucl. Phys. **21**, 255 (1975)].
[29] W. Dilg, W. Schantl, H. Vonach, and M. Uhl, Nucl. Phys. A **217**, 269 (1973).
[30] D. R. Chakrabarty, V. M. Datar, Suresh Kumar, E. T. Mirgule, H. H. Oza, and U. K. Pal, Phys. Rev. C **51**, 2942 (1995).
[31] Handbook for Calculations of Nuclear Reactions Data, IAEA, Vienna, Report No. IAEA-TECDOC-1024, 1998.
[32] G. Hansen and A. Jensen, Nucl. Phys. A **406**, 236 (1983).
[33] S. K. Pandit, A. Shrivastava, K. Mahata, V. V. Parkar, R. Palit, N. Keeley, P. C. Rout *et al.*, Phys. Rev. C **96**, 044616 (2017)
[34] P. C. Rout, D. R. Chakrabarty, V. M. Datar, S. Kumar, E. T. Mirgule, A. Mitra, V. Nanal, S. P. Behera, and V. Singh, Phys. Rev. Lett. **110**, 062501 (2013).
[35] J. Zhao, T. Niksic, and D. Vretenar, Phys. Rev. C **102**, 054606 (2020).
[36] S. M. Grimes, T. N. Massey, and A. V. Voinov, Phys. Rev. C **99**, 064331 (2019).